Kormilainen, Riku; Langi, Konsta; Lehtovuori, Anu; Viikari, Ville

Robust On-Body Antenna Based on Discretized Planar Surfaces

Published in:
2023 International Workshop on Antenna Technology, iWAT 2023

DOI:
10.1109/iWAT57058.2023.10171627

Published: 01/01/2023

Document Version
Peer-reviewed accepted author manuscript, also known as Final accepted manuscript or Post-print

Please cite the original version:
Kormilainen, R., Langi, K., Lehtovuori, A., & Viikari, V. (2023). Robust On-Body Antenna Based on Discretized Planar Surfaces. In *2023 International Workshop on Antenna Technology, iWAT 2023* IEEE. https://doi.org/10.1109/iWAT57058.2023.10171627

Robust On-Body Antenna Based on Discretized Planar Surfaces

Riku Kormilainen*, Konsta Langi*, Anu Lehtovuori*, Ville Viikari*
*Department of Electronics and Nanoengineering, Aalto University, Espoo, P.O. Box 15500, 00076 Aalto, Finland
ville.viikari@aalto.fi

***Abstract*—This paper presents a novel on-body antenna consisting of discretized metallic patch elements connected with lumped components. The antenna is designed to on-body application, and it could be placed, e.g., to the sling of the backpack. Since most of the human body is composed of water, it has a significant effect on antenna performance. The main effects include detuning of the antenna and a deteriorating radiation efficiency. The proposed antenna inherently resists the detuning effects as compared to a conventional antenna. Therefore, the antenna provides a robust operation in various user scenarios. The details of the structure and element values are optimized with a readily available method that enables the optimization of lumped components to improve the total efficiency. The results show that a 400 MHz bandwidth can be achieved with reasonable efficiency.**

***Index Terms*—optimization, planar antenna, wearable antenna, wireless body area network (WBAN)**

I. Introduction

Although mobile phones have remained the main means of wireless communication, different types of wearable antennas are emerging. It is estimated that they could be used for monitoring the human health and sports activity throughout the day or for recreational purposes [1]. However, a human body largely consisting of water imposes a great challenge to antenna design. Since water has a high dielectric constant and loss tangent, an antenna near the body typically has poor performance unless the effect of the body is properly considered.

Numerous locations near human body have been proposed to facilitate antennas, such as belts [2], clothes buttons [3], military berets [4], wrists [5], watches [6], glasses [7] and embedded in the textile [8], [9]. Since textile antennas must be flexible they are prone to bending and crumbling which may lead to frequency detuning as demonstrated in [8]. If an antenna is fabricated on a rigid substrate, this issue can be avoided. However, rigid antennas might detune due to another reasons. The distance between the antenna and the human can have a profound effect on the antenna impedance [10]. Finding a robust and wideband antenna might be challenging with conventional electromagnetic (EM) simulations.

Discretization has been used to facilitate the manipulation of an antenna structure by moving the computational load from electromagnetic simulations to circuit optimization through multiport models [11]–[14]. We propose to utilize this multiport antenna approach also in the case of wearable antennas.

The work of R. Kormilainen was supported by Aalto ELEC Doctoral School

In our approach, a patch antenna type of structure is discretized into separate metallic patches both on the ground and the antenna layer. Lumped components are placed between the patches to allow the surface current manipulation of the antenna structure. A readily available method exists [15] to find suitable values for lumped components. In the method, the discretized structure is first simulated as a multiport antenna, and then uses a genetic algorithm to find suitable lumped components. The optimized antenna structure is rigid and compact, and the performance is insensitive to detuning when varying the antenna distance from the human body, thus allowing its placement, for example on the sling of the backpack. Furthermore, the antenna achieves a reasonable bandwidth of 400 MHz.

II. Background and Generalized Design Flow

The idea to discretize the radiating surface of an antenna to better control the antenna properties has been discussed in [14]. The generalized modeling of a discretized antenna is shown in Fig. 1a. The antenna surface is divided into several connected pieces, and each connection is modeled as a feeding port in an EM-simulation. Thus, the resulting circuit model has several feeding ports. At least one port is chosen as a feeding port whereas the remaining ports are terminated with certain loads to control the current distribution of the radiating surface.

The generalized design flow of an arbitrary antenna is shown in Fig. 1b. As in all antenna design, the first step is to set goals for the antenna performance such as total efficiency over a certain band. Then, an antenna structure is chosen, and it is discretized and modeled as described previously. The antenna model is simulated, and the resulting antenna impedance matrices and port-specific far-fields are exported to construct a circuit model of the antenna. There are readily available sophisticated circuit models [12], [15] that enable the optimization of the loads to various design goals. The loads can be simple short and open circuits or lumped components.

We use the model for total efficiency [15] in this paper. The total efficiency of a multiport antenna at a single frequency can be stated as [15]

$$\eta_{\mathrm{tot}} = \frac{(\boldsymbol{a}_{\mathrm{F}})^{\mathrm{H}} \left((\mathbf{B}_{\mathrm{r}})^{-1}\right)^{\mathrm{H}} \mathbf{R}_{\mathrm{rad,r}} (\mathbf{B}_{\mathrm{r}})^{-1} \boldsymbol{a}_{\mathrm{F}}}{(\boldsymbol{a}_{\mathrm{F}})^{\mathrm{H}} \boldsymbol{a}_{\mathrm{F}}}, \tag{1}$$

where $\boldsymbol{a}_{\mathrm{F}}$ is a vector containing the port excitation signals, and $\mathbf{B}_{\mathrm{r}}$ and $\mathbf{R}_{\mathrm{rad,r}}$ are matrices dependent on the antenna impedance matrix $\mathbf{Z}_\mathrm{A}$ and the optimized load values. Furthermore, matrix $\mathbf{R}_\mathrm{rad,r}$ is dependent on the port-specific electric fields. In the case of a single feeding port, signal vector $\boldsymbol{a}_\mathrm{F}$ can be omitted from the equation. For further information on the theory, see [15].

The above equation allows the effective optimization of total efficiency with a suitable algorithm that can be implemented in a chosen programming language such as Python or MATLAB. Essentially, the equation is used to calculate the objective function of the chosen optimization algorithm. This optimization yields a suitable set of loads that, for example, maximizes the total efficiency over a bandwidth of 100 MHz at 2.5 GHz. When the optimization is finished, it is checked if the initial goals are achieved.

If all the goals are achieved, the antenna loads are realized using, for example, lumped elements and SMA connectors. If the goals are unobtainable, then there are two options to proceed with the optimization. The first option is to modify the simulated antenna structure and perform a new EM-simulation being close to traditional antenna design. The second option is to modify the design goals and perform a new optimization, and this is typically much faster than a new EM simulation. Moreover, applying different design goals yields important information on antenna operation, which can be used to modify the antenna structure to achieve better performance. In other words, the efficient design method enables analyzing the potential of the proposed antenna structure to different purposes.

III. Antenna Structure and Design Process

Next, we apply the described method to design a wideband antenna to on-body scenario. The antenna structure is shown in Fig. 2 with its dimensions and port numbering. The antenna consists of a Rogers RO4350B substrate with two metallic layers. Both the top and bottom layer consist of a 3 by 3 grid of metallic patches separated by a small gap. Adjacent patches are connected with discrete ports. Additionally the nearby patches are connected to the ground on the bottom layer. The antenna is fed with a 3.31 mm thick microstrip line corresponding to $50\,\Omega$ line impedance, and a total size of antenna is 60 mm x 60 mm x 1.5 mm. The total number of ports in the antenna is 28. The gap G between the human tissue and the antenna is varied.

Before the antenna optimization, a few design constraints are decided. The center frequency is set to 2.5 GHz, and the total antenna length/width is fixed to 31 mm. The length is based on the size of a conventional patch antenna at the center frequency. The gap between the antenna and the tissue is set to 5 mm since it might be a typical distance in a typical use case scenario. The feed port is shown in Fig. 2b by a red triangle. The remaining 27 ports are replaced with lumped elements such as capacitors, inductors, opens, and shorts. The goal in the optimization is to find proper components for these ports to maximize the total efficiency over a certain bandwidth.

The multi-port antenna is simulated with CST Microwave Studio within a frequency range from 2 to 3 GHz, and the obtained scattering parameters and electric far fields are exported into MATLAB. Then, the multi-port antenna is optimized with a mixed-integer genetic algorithm that is readily available in MATLAB via *Global Optimization Toolbox*. The objective function is calculated based on (1), and the function is defined every 25-MHz steps.

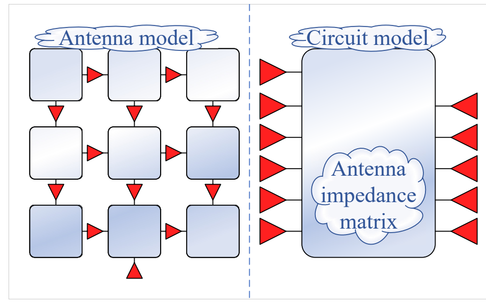

(a)

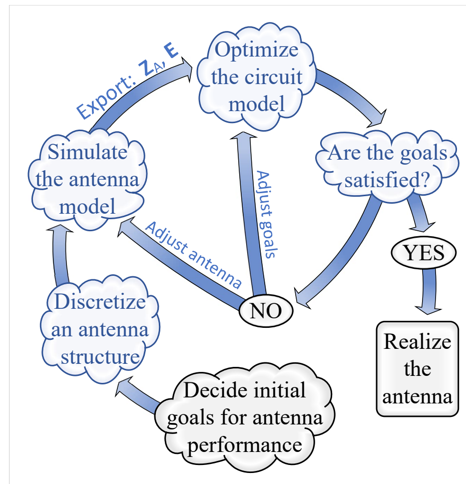

(b)

Fig. 1. Generalized (a) the simulation and circuit models, and (b) the design flow of a discretized antenna.

The proposed antenna is initially studied by using either lumped elements or solely short/open to realize the port connections between the patches and optimizing it to different bands. The optimization results are shown in Fig. 3. The antenna is optimized from 200 MHz up to 1000 MHz bands. Unsurprisingly, a more constrained bandwidth yields a higher total efficiency, and the lumped element connections enable better control of the total efficiency over the desired bands. As a good compromise between efficiency and the available bandwidth, the 400 MHz band is studied more thoroughly.

Since the antenna distance to the human tissue can vary in the user scenario (antenna attached to strap of the back pack), the robustness of the antenna is studied by comparing its performance at varying distances and optimization settings. The antenna is optimized for distances of 1, 3, and 5 mm by using either lumped elements or short/open connections, and the optimization results are shown in Fig. 4. In all the optimization cases, the antenna is robust to changes in the

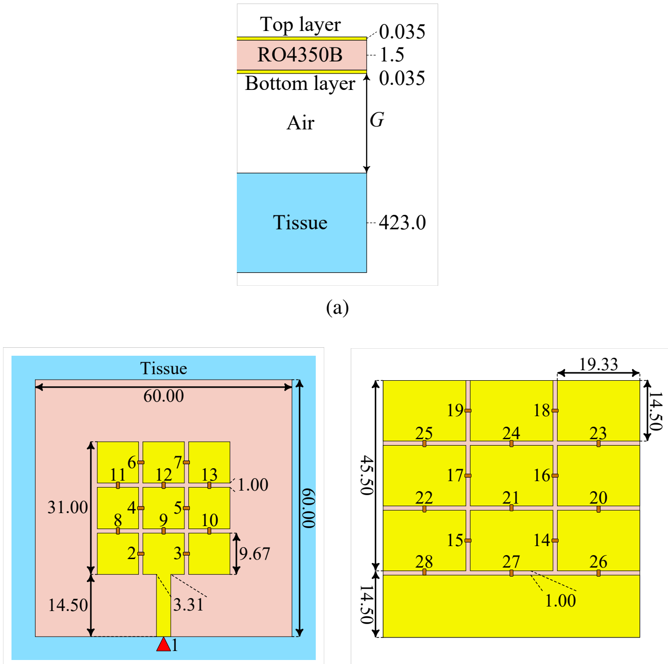

(a)

(b) (c)

Fig. 2. (a) Antenna and tissue cross-section, and antenna (b) bottom and (c) top layer showing dimensions and port numbering. All dimensions are in millimeters.

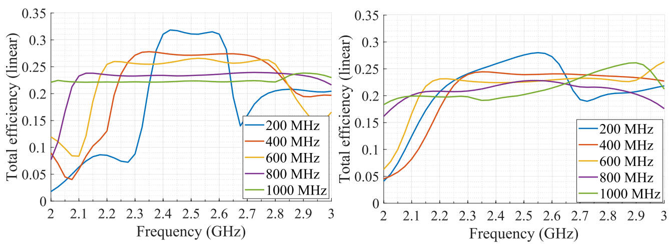

(a) (b)

Fig. 3. The total efficiency of the proposed antenna using (a) lumped elements or (b) short/open connections at a distance of 5 mm from the body with different optimized bands.

distance since the efficiency drop is constant when the distance between the antenna and the tissue decreases. However, the most robust results are achieved when the antenna is optimized at a 3 mm distance (Figs. 4c and 4d). Especially, the short/open realization has stable total efficiency curves which is evident from Fig. 4d. The lumped element solution is almost equally robust, but it has higher total efficiencies within all the distances. Therefore, an antenna optimized to 3 mm distance using lumped elements is chosen as the optimal solution.

IV. Final Results

As discussed, we choose the antenna optimized to a 400 MHz bandwidth when the antenna lies 3 mm away from the tissue by using lumped elements. The port configuration of the optimal antenna is shown in Table I, and the port numbering is the same as in Fig. 2. The table shows that connections are replaced with open connections, capacitors

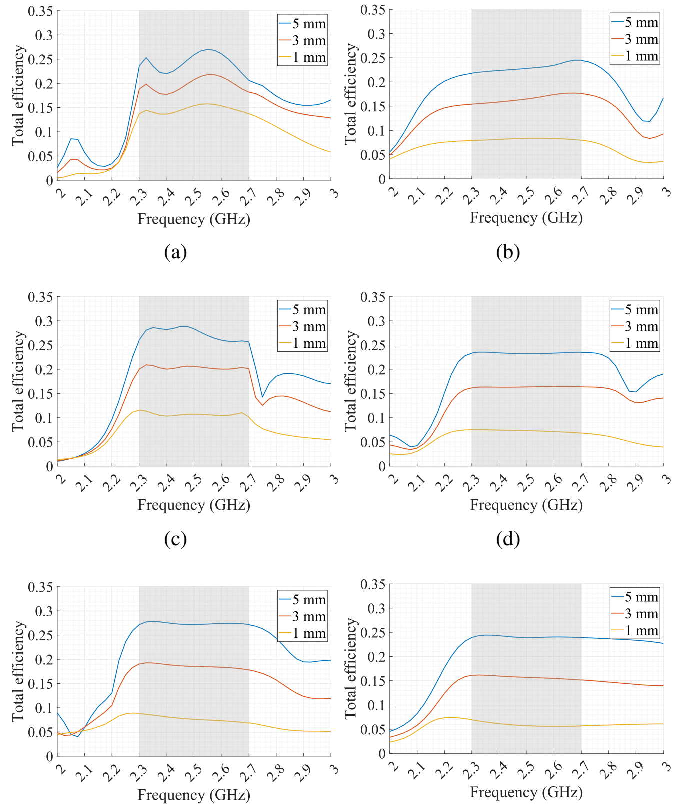

(a) (b)

(c) (d)

(e) (f)

Fig. 4. The total efficiency of the antenna at varying distances from the tissue. The proposed antenna has been optimized to 400 MHz bandwidth (a), (b) 1 mm, (c), (d) 3 mm and (e), (f) 5 mm away from the tissue by using (left column) lumped elements or (right column) short/open connections.

TABLE I
Component Configuration of the Proposed Antenna.

Port	Value	Port	Value	Port	Value	Port	Value
1	feed	8	3.4 nH	15	6.9 nH	22	2.8 pF
2	9.5 pF	9	open	16	3.4 pF	23	0.9 pF
3	open	10	open	17	25 nH	24	2.5 nH
4	9.7 pF	11	3.3 pF	18	1.9 pF	25	1.1 pF
5	open	12	2.5 pF	19	9.5 pF	26	5.9 pF
6	2.3 pF	13	2.3 pF	20	7.1 pF	27	3.8 pF
7	0.4 pF	14	open	21	6.3 pF	28	3.3 pF

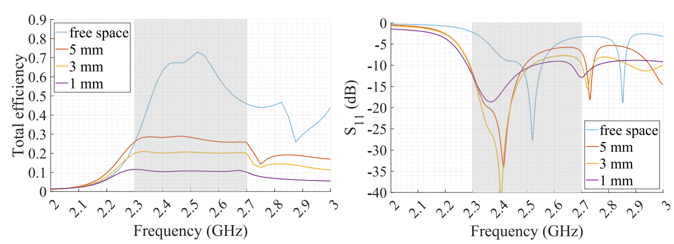

(a) (b)

Fig. 5. (a) The total efficiency and (b) the reflection coefficient of the optimal antenna at varying distances from the body.

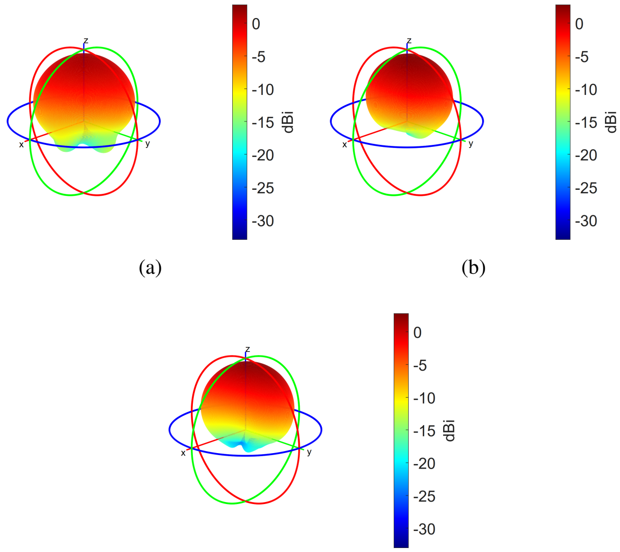

(a) (b) (c)

Fig. 6. The realized gain patterns of the proposed antenna 3 mm away from the tissue at frequencies of (a) 2.3, (b) 2.5, and (c) 2.7 GHz.

(0.4–9.7 pF), or inductors (2.5–25 nH). Note, that the used lumped elements are real models of Murata capacitors (series GJM1555C*) and inductors (series LQW15AN*80), and thus, the simulated results account for almost all the losses present in the antenna system.

The simulated total efficiency and reflection coefficient of the optimal antenna is shown in Fig. 5. The antenna has total efficiencies of 0.1, 0.2, and 0.25 at the three different distances. Furthermore, the antenna can function better when not near the tissue (free space). However, the reflection coefficient curves shows that there is a frequency shift when the tissue is completely removed. Varying the distance between the antenna and tissue from 1 to 5 mm seems to have a minor effect on the matching.

Furthermore, the realized gain pattern of the antenna is stable over the whole bandwidth (2.3–2.7 GHz) at a typical use case distance of 5 mm. The gain patterns at 2.3, 2.5, and 2.7 GHz are shown in Fig. 6, and all the patterns resemble those of a typical patch antenna.

V. Conclusions

The on-body antenna consisting of discretized metallic patch elements connected with lumped elements was presented. The antenna design is robust to tuning effects caused by proximity of human body, which makes it appropriate to wearable solutions. The results show that a 400 MHz bandwidth can be achieved with reasonable efficiency.

References

[1] A. Saboor, R. Ahmad, W. Ahmed, A. K. Kiani, Y. L. Moullec, and M. M. Alam, "On research challenges in hybrid medium-access control protocols for IEEE 802.15.6 WBANs," *IEEE Sensors Journal*, vol. 19, no. 19, pp. 8543–8555, 2019.

[2] R. Pei, M. P. Leach, E. G. Lim, Z. Wang, C. Song, J. Wang, W. Zhang, Z. Jiang, and Y. Huang, "Wearable EBG-backed belt antenna for smart on-body applications," *IEEE Transactions on Industrial Informatics*, vol. 16, no. 11, pp. 7177–7189, 2020.

[3] X. Y. Zhang, H. Wong, T. Mo, and Y. F. Cao, "Dual-band dual-mode button antenna for on-body and off-body communications," *IEEE Transactions on Biomedical Circuits and Systems*, vol. 11, no. 4, pp. 933–941, 2017.

[4] H. Lee, J. Tak, and J. Choi, "Wearable antenna integrated into military berets for indoor/outdoor positioning system," *IEEE Antennas and Wireless Propagation Letters*, vol. 16, pp. 1919–1922, 2017.

[5] K.-L. Wong, H.-J. Chang, C.-Y. Wang, and S.-Y. Wang, "Very-low-profile grounded coplanar waveguide-fed dual-band WLAN slot antenna for on-body antenna application," *IEEE Antennas and Wireless Propagation Letters*, vol. 19, no. 1, pp. 213–217, 2020.

[6] S.-W. Su and Y.-T. Hsieh, "Integrated metal-frame antenna for smartwatch wearable device," *IEEE Transactions on Antennas and Propagation*, vol. 63, no. 7, pp. 3301–3305, 2015.

[7] S. Hong, S. H. Kang, Y. Kim, and C. W. Jung, "Transparent and flexible antenna for wearable glasses applications," *IEEE Transactions on Antennas and Propagation*, vol. 64, no. 7, pp. 2797–2804, 2016.

[8] B. Hu, G.-P. Gao, L.-L. He, X.-D. Cong, and J.-N. Zhao, "Bending and on-arm effects on a wearable antenna for 2.45 GHz body area network," *IEEE Antennas and Wireless Propagation Letters*, vol. 15, pp. 378–381, 2016.

[9] T. T. Le, Y.-D. Kim, and T.-Y. Yun, "A triple-band dual-open-ring high-gain high-efficiency antenna for wearable applications," *IEEE Access*, vol. 9, pp. 118 435–118 442, 2021.

[10] S. M. Abbas, K. P. Esselle, L. Matekovits, M. Rizwan, and L. Ukkonen, "On-body antennas: Design considerations and challenges," in *2016 URSI International Symposium on Electromagnetic Theory (EMTS)*, 2016, pp. 109–110.

[11] D. Rodrigo and L. Jofre, "Frequency and radiation pattern reconfigurability of a multi-size pixel antenna," *IEEE Transactions on Antennas and Propagation*, vol. 60, no. 5, pp. 2219–2225, 2012.

[12] S. Song and R. D. Murch, "An efficient approach for optimizing frequency reconfigurable pixel antennas using genetic algorithms," *IEEE Transactions on Antennas and Propagation*, vol. 62, no. 2, pp. 609–620, 2014.

[13] S. Soltani, P. Lotfi, and R. D. Murch, "Design and optimization of multiport pixel antennas," *IEEE Transactions on Antennas and Propagation*, vol. 66, no. 4, pp. 2049–2054, 2018.

[14] R. Kormilainen, J.-M. Hannula, T. O. Saarinen, A. Lehtovuori, and V. Viikari, "Realizing optimal current distributions for radiation efficiency in practical antennas," *IEEE Antennas and Wireless Propagation Letters*, vol. 19, no. 5, pp. 731–735, 2020.

[15] R. Kormilainen, *Design and Optimization Methods for Multiport Antennas*. Doctoral Thesis, Aalto University, Finland, 2022.